

Structure-property relations for polymer melts: comparison of linear low-density polyethylene and isotactic polypropylene

A.D. Drozdov¹, A. Al-Mulla*² and R.K. Gupta¹

¹*Department of Chemical Engineering, West Virginia University, WV, USA*

²*Department of Chemical Engineering, Kuwait University, Safat, Kuwait*

(Received July 2, 2012, Revised August 20, 2012, Accepted September 5, 2012)

Abstract. Results of isothermal torsional oscillation tests are reported on melts of linear low density polyethylene and isotactic polypropylene. Prior to rheological tests, specimens were annealed at various temperatures ranging from $T_a = 180$ to 310°C for various amounts of time (from 30 to 120 min). Thermal treatment induced degradation of the melts and caused pronounced decreases in their molecular weights. With reference to the concept of transient networks, constitutive equations are developed for the viscoelastic response of polymer melts. A melt is treated as an equivalent network of strands bridged by junctions (entanglements and physical cross-links). The time-dependent response of the network is modelled as separation of active strands from and merging of dangling strands with temporary nodes. The stress-strain relations involve three adjustable parameters (the instantaneous shear modulus, the average activation energy for detachment of active strands, and the standard deviation of activation energies) that are determined by matching the dependencies of storage and loss moduli on frequency of oscillations. Good agreement is demonstrated between the experimental data and the results of numerical simulation. The study focuses on the effect of molecular weight of polymer melts on the material constants in the constitutive equations.

Keywords: thermal properties; isotactic polypropylene; linear low-density polyethylene; molecular weight; viscoelasticity; thermal degradation

1. Introduction

This paper is concerned with the effects of the mass-average molecular weight and the microstructure of chains on the viscoelastic behavior of polyolefins in conventional shear oscillation tests. The choice of iPP for the experimental analysis is explained by numerous industrial applications of this semicrystalline polymer (oriented films for packaging, reinforcing fibres, non-woven fabrics, pipes, etc.).

The experimental part focuses on the response of injection-molded isotactic polypropylene (iPP) and linear low-density polyethylene (LLDPE). The choice of these polymers for the investigation is explained by (1) their numerous industrial applications and (2) the variety of their molecular architectures (corresponding to the same structure of backbones), ranging from highly branched chains with helix conformation in iPP to linear chains with short branches and planar conformation in LLDPE (Kim 2000). The difference in the chain structure of these polyolefins is reflected by the

*Corresponding author, Ph. D., E-mail: a.almulla1@ku.edu.kw

difference in their crystalline morphology below the melting temperature. Crystalline phase in isotactic polypropylene contains mainly monoclinic polymorphs and “smectic” mesophase (Lijima 2000), whereas crystalline regions in linear low-density polyethylene are formed by orthorhombic crystallites. A unique feature of iPP is the lamellar cross-hatching: development of transverse lamellae oriented in the direction perpendicular to the direction of radial lamellae (Lijima 2000), while the characteristic feature of LLDPE is that the average size of lamellae and their curvature are strongly affected by molecular weight and the degree of branching of chains (Matsuda 2001).

The effect of molecular weight and chain structure on the crystalline morphology and thermal and rheological properties of polyolefins has attracted substantial attention in the past decade. It was demonstrated that branching of chains (1) results in reductions in the glass transition T_g and melting T_m temperatures (Mäder 2000), (2) implies a growth of free-volume holes and a decrease in the density of packing of chains (Dlubek 2002) and (3) increases the melt viscosity, storage modulus, strength of polymer melts (Gao 2002), and the activation energy for thermo-activated processes (Combs 1969). An increase in the molecular weight results in the growth of melting temperature (Tiemblo 2002), a decrease in the degree of crystallinity, an increase in the yield stress and brittle-ductile transition in the fracture mode (Pérez 2003).

The influence of molecular weight on the time-dependent behavior of polymer melts in conventional shear oscillation tests has been investigated in (Barakos 1996, Wang 1996, Carrot 1996, Berzin 2001, Fujiyama 2002, Drozdov 2005). It was found that the growth of mass-average molecular weight induces (1) an increase in storage and loss moduli (Carrot 1996, Berzin 2001, Drozdov 2005), (2) a pronounced growth of the average relaxation time (Berzin 2001), an increase in the crossover frequency (the frequency at which storage and loss moduli coincide) (Barakos 1996), a reduction in the critical shear rate (Combs 1969), and the growth of the first normal difference of stresses (Barakos 1996).

Five approaches are conventionally employed for the modification of polymer melts: (1) oxidative degradation with peroxide (Barakos 1996, Wang 1996, Carrot 1996, Berzin 2001), (2) radiative degradation that causes cross-linking of chains and formation of a network structure (Gao 2002), (3) mechanical degradation by severe shear flow that induces disentanglement of chains (Van 1994, Kim 1998), (4) controlled metallocene catalysis (Eckstein 1997, Fujiyama 2002) and (5) addition of small amounts of chains with high molecular weight to a low-molecular-weight melt (Sugimoto 2001). In this study, we use thermal degradation of melts (annealing at elevated temperatures) as a means for changes in molecular weight. This method does not require special equipment (like controlled polymerization and radiative degradation), but ensures a noticeable decrease in the molecular weight (unlike mechanical degradation, which preserves the distribution of molecular weights practically unchanged (Prooyen 1994)). An advantage of thermal degradation compared to chemical modification with peroxide is that the evolution of molecular weight occurs relatively slowly (with the characteristic time of tens of minutes versus seconds), which implies that the kinetics of degradation can be studied in detail. However, we do not dwell on this issue in the present work: the kinetics of thermal and thermo-oxidative degradation have been recently studied in (Fayolle 2002, Gao 2003) for polypropylene and in (Rangarajan 1998, Kumar 2002) for polyethylene.

The objective of this study is three-fold: (1) to report experimental data in torsional oscillation tests on LLDPE and iPP annealed at various temperatures T_a for various amounts of time t_a , (2) to develop constitutive equations for the viscoelastic response of a polymer melt and to find material constants in the stress-strain relations by fitting the observations and (3) to compare the effects of molecular weight on the adjustable parameters for two polyolefins with different architectures of chains.

To make the model tractable from the mathematical standpoint, we adopt the homogenization hypothesis. According to it, a complicated micro-structure of a polymer melt is replaced by an equivalent phase, whose response captures essential features of the mechanical behavior. With reference to (Green 1946, Yamamoto 1956, Lodge 1968, Tanaka 1992), a transient network of strands bridged by temporary junctions (entanglements and physical cross-links) is chosen as the equivalent phase. According to the concept of transient networks, active strands separate from their junctions at random times being excited by thermal fluctuations, and dangling strands merge with the network. Following (Drozdov 2003), we assume the network to be strongly heterogeneous in the sense that different junctions have different activation energies for detachment of strands. The concept of temporary networks was employed to describe the time-dependent behavior of polypropylene in (Drozdov 2003, Sweeney 1999) and that of polyethylene in (Drozdov 2003). The previous studies did not, however, pay much attention to the effect of molecular weight on material parameters in the constitutive equations. The aim of this work is to evaluate the influence of mass-average molecular weight on (1) the concentration of active strands in an equivalent network and (2) the distribution function for temporary junctions with various activation energies.

The exposition is organized as follows. First, experimental data in torsional oscillation tests are reported on annealed specimens, and their mass-average molecular weights are determined by using observations for complex viscosity. We proceed with the derivation of stress-strain relations for an heterogeneous transient network at three-dimensional deformations with small strains. The constitutive equations involve three material constants that are found by matching the data for the storage and loss moduli as functions of the frequency of oscillations. Finally, we establish correlations between the adjustable parameters in the stress-strain relations and mass average molecular weights of the melts and discuss the physical meaning of these relationships.

2. Experimental procedure

Linear low-density polyethylene Petrothene GA 584 (density 0.929 g/cm^3 , melt flow rate 105 g/10 min) was supplied by Equistar Chemicals. Isotactic polypropylene PP 1012 (density 0.906 g/cm^3 , melt flow rate 1.2 g/10 min) was purchased from BP Amoco Polymers, Inc.

Granules were dried overnight at the temperature $T = 100^\circ\text{C}$. Circular plates with diameter 64 mm and thickness 3 mm were molded in injection-molding machine Battenfeld 1000/315 CDC (Battenfeld). Circular specimens for rheological tests (with diameter 30 mm) were cut from the plates.

To evaluate the melting temperature T_m , DSC (differential scanning calorimetry) measurements were performed by using DSC 910S apparatus (TA Instruments). The calorimeter was calibrated with indium as a standard. Two specimens of each polyolefin with weights of approximately 15 mg were tested with a heating rate of 10 K/min from room temperature to 200°C under nitrogen. The melting temperatures $T_m = 131$ (LLDPE) and $T_m = 172^\circ\text{C}$ (iPP) were determined as the points corresponding to the peaks on the melting curves.

Rheological tests were performed by using RMS-800 rheometric mechanical spectrometer with parallel disks (diameter 25 mm , gap length 2 mm) at the temperatures $T = 140$ (LLDPE) and $T = 230^\circ\text{C}$ (iPP) that exceed the melting temperatures of the polymers under investigation. The shear storage modulus G' , the shear loss modulus G'' and the modulus of complex viscosity η were measured in oscillation tests (the frequency-sweep mode) with the amplitude of 15% and various

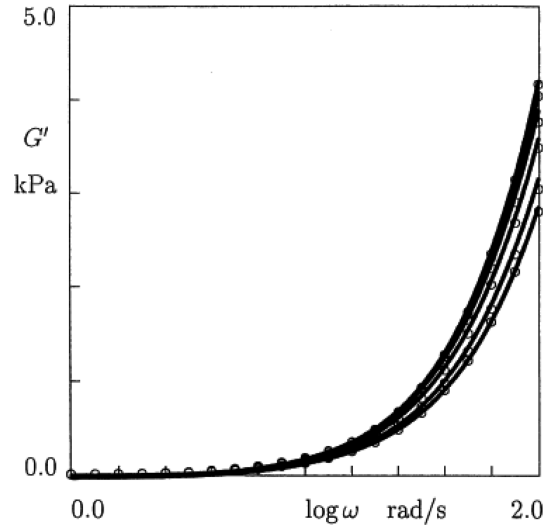


Fig. 1 The storage modulus G' versus frequency ω . Circles: experimental data in torsional oscillation tests at the temperature $T = 140^\circ\text{C}$ on LLDPE annealed at temperature T_a °C for t_a min: $T_a = 140$, $t_a = 0$; $T_a = 180$, $t_a = 60$; $T_a = 200$, $t_a = 60$; $T_a = 220$, $t_a = 30$; $T_a = 240$, $t_a = 30$; $T_a = 260$, $t_a = 30$, from top to bottom, respectively. Solid lines: results on numerical simulation

frequencies ω ranging from 1.0 to 100 (LLDPE) and from 0.1 to 100 rad/s (iPP). The choice of the amplitude of oscillations was driven by the following requirements: (1) mechanical tests were performed in the region of linear viscoelasticity and (2) the torque was less than its ultimate value 0.2 N.m. The limitation on the minimum frequency of oscillations was imposed by the condition that the torque exceeded its minimum value 2.0×10^4 N.m. To check that the storage and loss moduli were not affected by the strain amplitude, several tests were repeated with the amplitude of 5%; no changes in dynamic moduli were observed. The temperature in the chamber was controlled with a standard thermocouple that showed that the temperature of specimens remained practically constant (with the accuracy of $\pm 0.5^\circ\text{C}$).

Prior to oscillatory tests, LLDPE samples were annealed in the spectrometer at the temperatures $T_a = 180$ and 200°C for $t_a = 60$ min, and at the temperatures $T_a = 220$, 240 and 260°C for $t_a = 30$ min. After thermal treatment of each specimen (with the gap length of 3 mm), the temperature was decreased to the test temperature $T = 140^\circ\text{C}$, the specimen was thermally equilibrated (during 5 min), the gap length was reduced to 2 mm, an extraneous material was carefully removed, and the storage and loss moduli and the complex viscosity were measured at various frequencies ω starting from the lowest one. Each test was performed on a new specimen.

The same procedure of testing was used for iPP samples (with the test temperature $T = 230^\circ\text{C}$) annealed at $T_a = 190^\circ\text{C}$ for $t_a = 30, 60, 90$ and 120 min and annealed at $T_a = 250, 270, 290$ and 310°C for $t_a = 60$ min.

We suppose that squeezing of samples between plates of the spectrometer and removal of the extraneous material substantially reduced the effect of thermo-oxidative degradation (compared to that of thermal degradation) on the mechanical response, because the major part of the material where oxidative degradation occurred was taken away (about one third of the initial mass of each specimen). However, we cannot exclude entirely the effect of diffusion of oxygen to the central

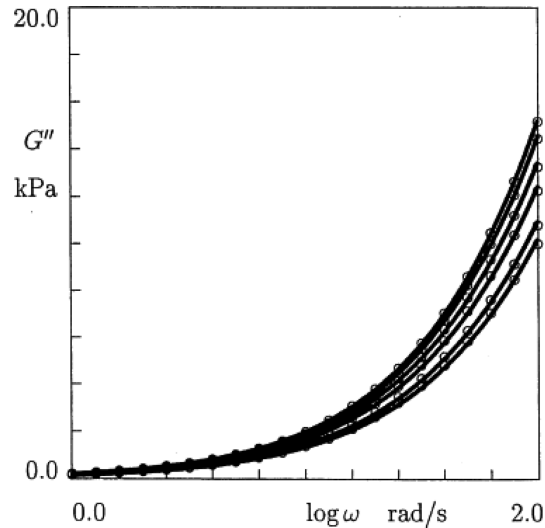


Fig. 2 The loss modulus G'' versus frequency ω . Circles: experimental data in torsional oscillation tests at the temperature $T = 140^\circ\text{C}$ on LLDPE annealed at temperature T_a °C for t_a min: $T_a = 140, t_a = 0$; $T_a = 180, t_a = 60$; $T_a = 200, t_a = 60$; $T_a = 220, t_a = 30$; $T_a = 240, t_a = 30$; $T_a = 260, t_a = 30$, from top to bottom, respectively. Solid lines: results on numerical simulation

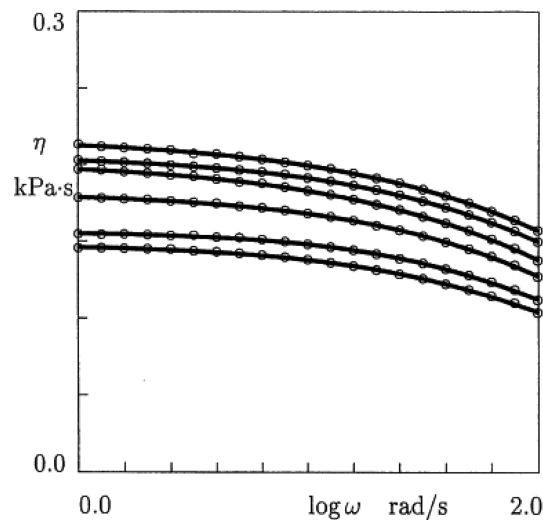


Fig. 3 The complex viscosity η versus frequency ω . Circles: experimental data in torsional oscillation tests at the temperature $T = 140^\circ\text{C}$ on LLDPE annealed at T_a °C for t_a min: $T_a = 140, t_a = 0$; $T_a = 180, t_a = 60$; $T_a = 200, t_a = 60$; $T_a = 220, t_a = 30$; $T_a = 240, t_a = 30$; $T_a = 260, t_a = 30$, from top to bottom, respectively. Solid lines: results on numerical simulation

parts of the samples, in particular, at the highest temperatures ($T_a = 290$ and 310°C) used in the experiments (Drozdov 2003).

The storage G' and loss G'' moduli, as well as the modulus of complex viscosity η are depicted versus the logarithm ($\log = \log_{10}$) of frequency ω in Figs. 1 to 3 for LLDPE and in Figs. 4 to 9 for

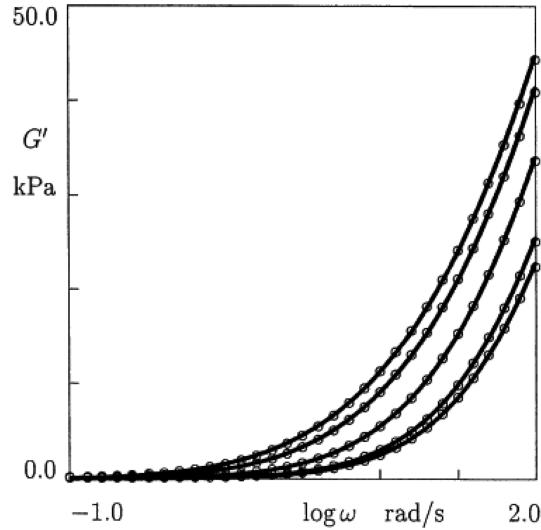


Fig. 4 The storage modulus G' versus frequency ω . Circles: experimental data in torsional oscillation tests at the temperature $T = 230^\circ\text{C}$ on iPP annealed at $T_a = 190^\circ\text{C}$ for $t_a = 0, 30, 60, 90$ and 120 min, from top to bottom, respectively. Solid lines: results on numerical simulation

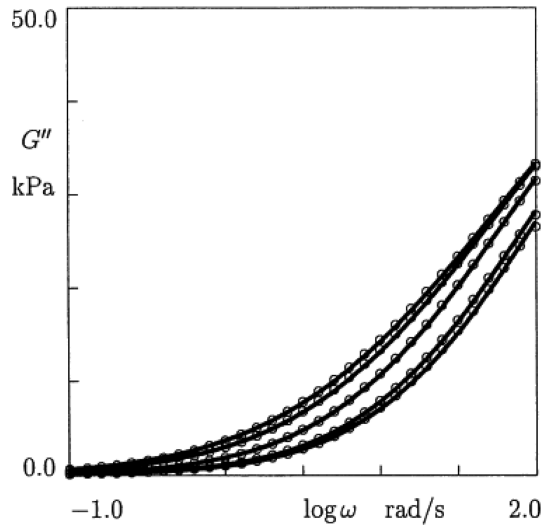


Fig. 5 The loss modulus G'' versus frequency ω . Circles: experimental data in torsional oscillation tests at the temperature $T = 230^\circ\text{C}$ on iPP annealed at $T_a = 190^\circ\text{C}$ for $t_a = 0, 30, 60, 90$ and 120 min, from top to bottom, respectively. Solid lines: results on numerical simulation

iPP. Conventional semi-logarithmic plots are used to characterize changes in these quantities with frequency.

According to Figs. 1 to 9, the dependencies of storage and loss moduli on frequency of oscillations have similar shapes for both polymers, whereas the shapes of the graphs $\eta(\omega)$ substantially differ from each other. Given an annealing time t_a and an annealing temperature T_a , the

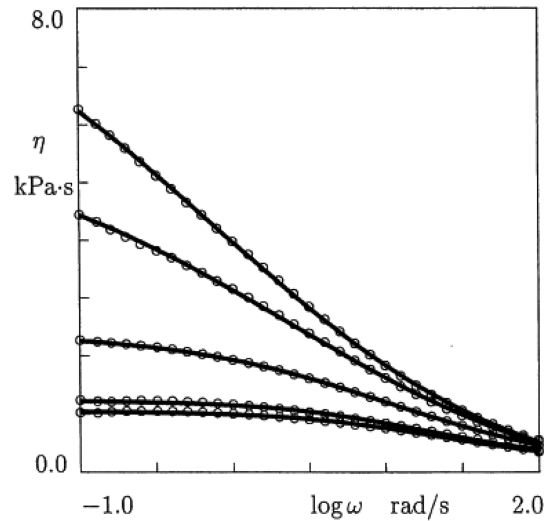


Fig. 6 The complex viscosity η versus frequency ω . Circles: experimental data in torsional oscillation tests at the temperature $T = 230^\circ\text{C}$ on iPP annealed at $T_a = 190^\circ\text{C}$ for $t_a = 0, 30, 60, 90$ and 120 min, from top to bottom, respectively. Solid lines: results on numerical simulation

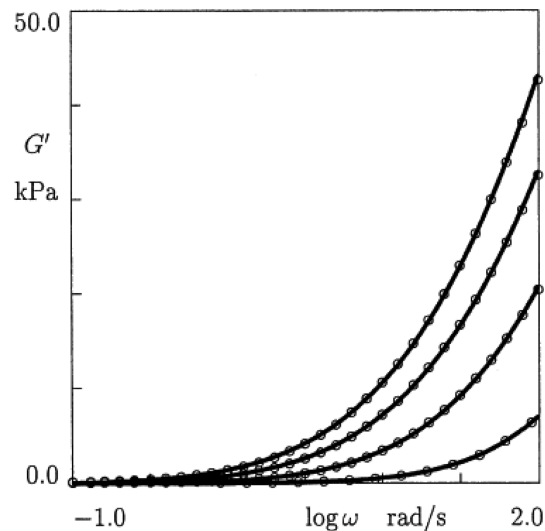


Fig. 7 The storage modulus G' versus frequency ω . Circles: experimental data in torsional oscillation tests at the temperature $T = 230^\circ\text{C}$ on iPP annealed for $t_a = 60$ min at $T_a = 250, 270, 290$ and 310°C , from top to bottom, respectively. Solid lines: results on numerical simulation

storage modulus G' and the loss modulus G'' strongly increase with frequency, whereas the complex viscosity η slightly decreases with ω for LLDPE and it is strongly reduced for iPP. For a fixed frequency ω , the dynamic moduli and the modulus of complex viscosity decrease with annealing temperature T_a and annealing time t_a . The reduction in G' and G'' is quite comparable for LLDPE, whereas the relative decrease in G' substantially exceeds that in G'' for iPP.

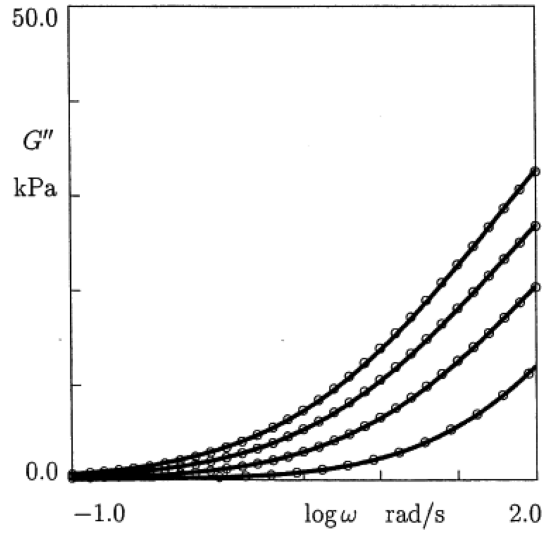


Fig. 8 The loss modulus G'' versus frequency ω . Circles: experimental data in torsional oscillation tests at the temperature $T = 230^\circ\text{C}$ on iPP annealed for $t_a = 60$ min at $T_a = 250, 270, 290$ and 310°C , from top to bottom, respectively. Solid lines: results on numerical simulation

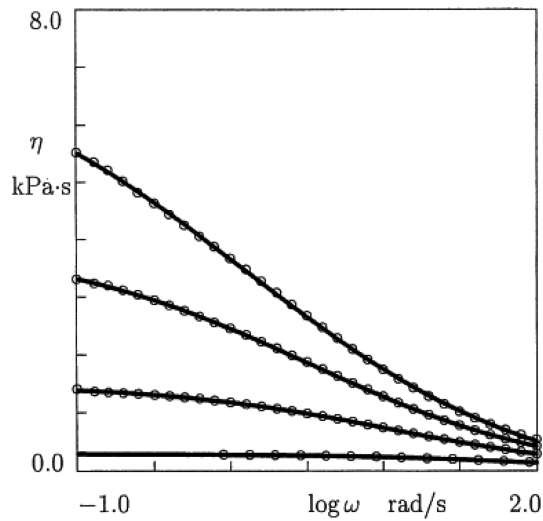


Fig. 9 The complex viscosity η versus frequency ω . Circles: experimental data in torsional oscillation tests at the temperature $T = 230^\circ\text{C}$ on iPP annealed for $t_a = 60$ min at $T_a = 250, 270, 290$ and 310°C , from top to bottom, respectively. Solid lines: results on numerical simulation

3. Theory

3.1 Evaluation of molecular weight

To assess changes in molecular weight induced by thermal degradation of the polymer melts, the

observations for $\eta(\omega)$ depicted in Figs. 3, 6 and 9 are approximated by the Cross model

$$\eta(\omega) = \eta_\infty + \frac{\Delta\eta}{1 + (\tau\omega)^\alpha}. \quad (1)$$

Here η_∞ is the high-frequency complex viscosity, η_0 is the zero-frequency complex viscosity, $\Delta\eta = \eta_0 - \eta_\infty$, and α and T are adjustable parameters.

Each curve $\eta(\omega)$ is fitted separately. To find the constants $\eta_\infty, \Delta\eta, \alpha$ and τ in Eq. (1), we fix some intervals $[0, \alpha_{\max}]$ and $[0, \tau_{\max}]$, where the “best-fit” parameters α and τ are assumed to be located, and divide these intervals into J subintervals by the points $\alpha^{(i)} = i\Delta\alpha$ and $\tau^{(j)} = j\Delta\tau$ ($i, j = 1, \dots, J-1$) with $\Delta\alpha = \alpha_{\max}/J$ and $\Delta\tau = \tau_{\max}/J$. For any pair $\{\alpha^{(i)}, \tau^{(j)}\}$, the coefficients η_∞ and $\Delta\eta$ in Eq. (1) are found by the least-squares method from the condition of minimum of the function.

$$F = \sum_{\omega_m} [\eta_{\text{exp}}(\omega_m) - \eta_{\text{num}}(\omega_m)]^2,$$

where the sum is calculated over all experimental points ω_m depicted in Figs. 3, 6 and 9, η_{exp} is the complex viscosity measured in a test, and η_{num} is given by Eq. (1). The “best-fit” parameters α and τ are determined from the condition of minimum of the function F on the set $\{\alpha^{(i)}, \tau^{(j)}\}$. After finding the “best-fit” values $\alpha^{(i)}$ and $\tau^{(j)}$, this procedure is repeated twice for the new intervals $[\alpha^{(i-1)}, \alpha^{(i+1)}]$ and $[\tau^{(j-1)}, \tau^{(j+1)}]$, to ensure an acceptable accuracy of fitting. Figs. 3, 6 and 9 demonstrate good agreement between the experimental data and the results of numerical simulation.

After finding the zero-frequency viscosity η_0 , the mass-average molecular weight M_w is determined by the conventional equation (Horrocks 1994)

$$\frac{\eta_0}{\eta_0^{\text{ref}}} = \left(\frac{M_w}{M_w^{\text{ref}}} \right)^{3.4} \quad (2)$$

where η_0^{ref} and M_w^{ref} are the zero-frequency viscosity and the mass-average molecular weight of a reference (not subjected to thermal treatment) specimen. The ratio of mass-average molecular weights

$$d_w = \frac{M_w}{M_w^{\text{ref}}}$$

is found from Eq. (2) by using the experimental data for η_0 . This method of determining the ratio of mass-average molecular weights of polypropylene was previously used in (Sugimoto 2001).

For each annealing time t_a and annealing temperature τ_a , we (1) calculate the material constants α and τ in Eq. (1) by matching the observations depicted in Figs. 3, 6 and 9, (2) find the ratio of mass-average molecular weights d_w from Eqs. (1) and (2) and (3) plot the adjustable parameters α and τ versus d_w in Figs. 10 to 13. The experimental data for the dimensionless exponent α are approximated by the linear function.

$$\alpha = \alpha_0 - \alpha_1 d_w, \quad (3)$$

where the coefficients α_i ($i = 0, 1$) are found by the least-squares technique. Figs. 10 and 11 show that Eq. (3) provides reasonable quality of matching the observations. To evaluate the influence of mass-average molecular weight d_w on the exponent α , it is convenient to present Eq. (3) in the form

$$\alpha = \alpha_* [1 + z_\alpha (1 - d_w)],$$

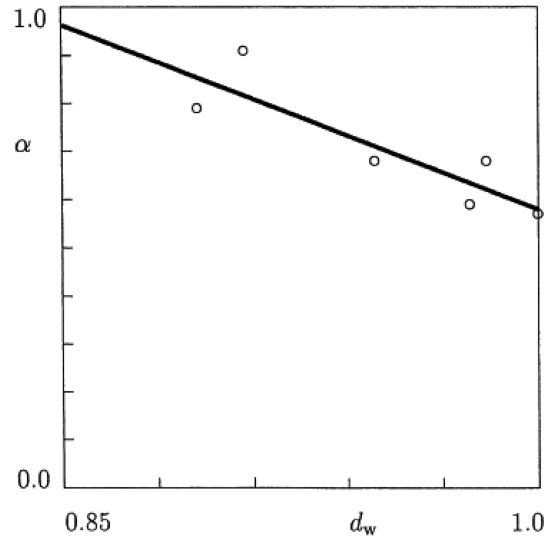


Fig. 10 The dimensionless exponent α versus the ratio of mass-average molecular weights d_w . Circles: treatment of observations in torsional oscillation tests on LLDPE. Solid line: approximation of the experimental data by Eq. (3) with $\alpha_0 = 3.14$ and $\alpha_1 = 2.56$

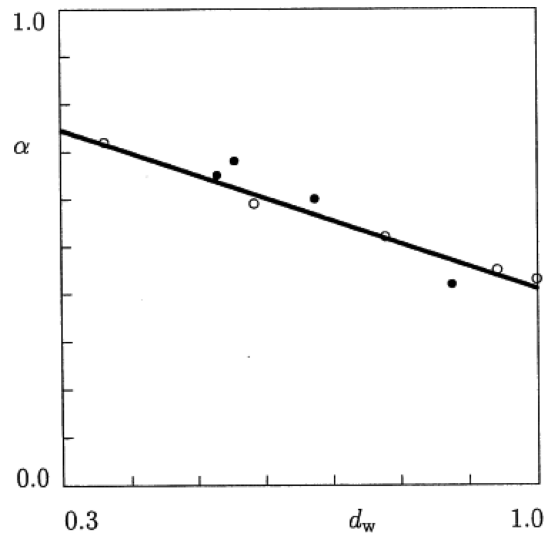


Fig. 11 The dimensionless exponent α versus the ratio of mass-average molecular weights d_w . Circles: treatment of observations in torsional oscillation tests on iPP. Solid line: approximation of the experimental data by Eq. (3) with $\alpha_0 = 0.89$ and $\alpha_1 = 0.48$

where $\alpha_0 = \alpha_*(1+z_\alpha)$ and $\alpha_1 = \alpha_*z_\alpha$. We calculate the coefficient z_α by using the experimental data presented in Figs. 10 and 11 and obtain $z_\alpha = 4.41$ for LLDPE and $z_\alpha = 1.16$ for iPP. This implies that the influence of molecular weight on α is noticeably more pronounced for linear low-density polyethylene than for isotactic polypropylene.

The experimental data for the characteristic time τ are fitted by the phenomenological relation

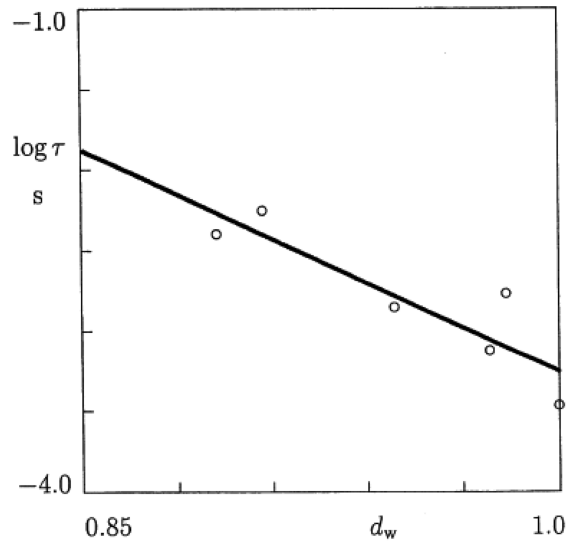


Fig. 12 The characteristic time τ versus the ratio of mass-average molecular weights d_w . Circles: treatment of observations in torsional oscillation tests on LLDPE. Solid line: approximation of the experimental data by Eq. (4) with $\tau_0 = 5.94$ and $\tau_1 = -9.19$

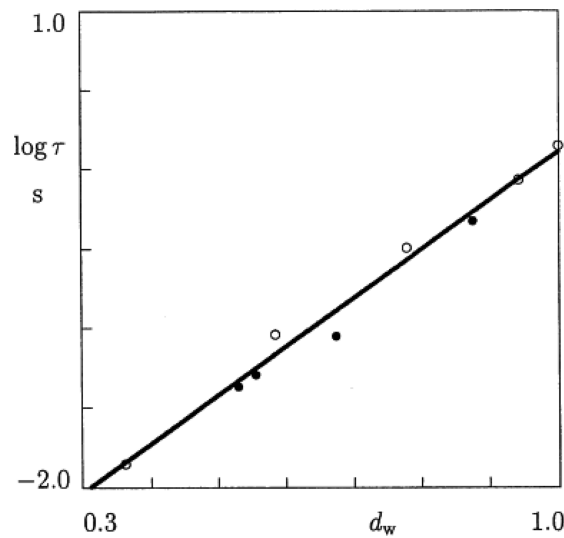


Fig. 13 The characteristic time τ versus the ratio of mass-average molecular weights d_w . Circles: treatment of observations in torsional oscillation tests on iPP. Solid line: approximation of the experimental data by Eq. (4) with $\tau_0 = -2.95$ and $\tau_1 = 3.06$

$$\log \tau = \tau_0 + \tau_1 d_w, \quad (4)$$

where the coefficients $\tau_i (i=0,1)$ are determined by the least-squares method. Figs. 12 and 13 demonstrate that Eq. (4) ensures an acceptable approximation of the observations. These figures reveal quite a different behavior of τ . It strongly decreases with molecular weight for LLDPE and

exponentially increases with M_w for iPP. The characteristic time τ for iPP substantially exceeds that for LLDPE, which explains the difference between the shapes of the curves depicted in Fig. 3, on the one hand, and in Figs. 6 and 9, on the other.

3.2 Constitutive equations

Our aim now is to approximate the experimental data for storage and loss moduli of the melts annealed at various temperatures T_a for various amounts of time t_a . For this purpose, we derive constitutive equations for the viscoelastic response of a polymer melt at three-dimensional deformations with small strains, simplify these equations for steady shear oscillations, and find adjustable parameters in the stress-strain relations by matching the observations depicted in Figs. 1, 2, 4, 5, 7 and 8.

Our analysis is based on the assumption that the characteristic time for thermal degradation (of the order of a few hours) substantially exceeds that for relaxation of stresses in a polymer melt (of the order of a few seconds), which implies that degradation of the melts during the rheological tests is disregarded.

A polymer melt is modelled as an equivalent network of strands bridged by temporary junctions (entanglements and physical cross-links whose life-times do not exceed the characteristic time of the rheological tests). A strand whose ends are linked to contiguous junctions is treated as an active one. When an end of an active strand separates from a junction, the strand is transformed into the dangling state. When a free end of a dangling strand captures a nearby junction, the strand returns into the active state. Separation of active strands from their junctions and merging of dangling strands with the network occur at random times when the strands are excited by thermal fluctuations. According to the theory of thermally-activated processes, the rate of detachment of strands from temporary junctions Γ is governed by the equation

$$\Gamma = \Gamma_0 \exp\left(-\frac{\bar{v}}{k_B T}\right),$$

where Γ_0 is the attempt rate (the number of separation events per strand per unit time), k_B is Boltzmann's constant, T is the absolute temperature, and $\bar{v} \geq 0$ is the activation energy for separation of an active strand. The coefficient Γ_0 is independent of the activation energy \bar{v} and is determined by the current temperature T only. Confining ourselves to isothermal processes at a reference temperature T^{ref} and introducing the dimensionless activation energy $v = \bar{v}/(k_B T^{ref})$, we present the Eyring equation in the form

$$\Gamma(v) = \Gamma_0 \exp(-v). \quad (5)$$

With reference to (Drozdov 2003), we assume that different junctions are characterized by different dimensionless activation energies v . The distribution of active strands in a transient network is determined by the number of active strands per unit mass N_a and the distribution function $p(v)$. The quantity $N_a P(v) dv$ equals the number of active strands per unit mass linked to junctions with the dimensionless activation energies u belonging to the interval $[v, v + dv]$.

Separation of active strands from temporary junctions and merging of dangling strands with the network are entirely described by the function $n(t, \tau, v)$ that equals the number (per unit mass) of active strands at time $t \geq 0$ linked to temporary junctions with activation energy v which have last merged with the network before instant $\tau \in [0, t]$.

The quantity $n(t, t, v)$ equals the number of active strands (per unit mass) with the activation energy v at time t ,

$$n(t, t, v) = N_{ap}(v). \quad (6)$$

The function

$$\gamma(\tau, v) = \left. \frac{\partial n}{\partial T}(t, \tau, v) \right|_{t=\tau} \quad (7)$$

determines the rate of reformation for dangling chains: the amount $\gamma(\tau, v)d\tau$ equals the number of dangling strands (per unit mass) that merge with temporary junctions with activation energy v within the interval $[\tau, \tau + d\tau]$. The quantity

$$\frac{\partial n}{\partial \tau}(t, \tau, v)d\tau$$

is the number of these strands that have not separated from their junctions during the interval $[\tau, t]$. The amount

$$-\frac{\partial n}{\partial t}(t, 0, v)dt$$

is the number of active strands (per unit mass) that detach (for the first time) from the network within the interval $[t, t + dt]$, while the quantity

$$-\frac{\partial^2 n}{\partial t \partial \tau}(t, \tau, v)dtd\tau$$

equals the number of strands (per unit mass) that have last merged with the network within the interval $[\tau, \tau + d\tau]$ and separate from the network (for the first time after their attachment) during the interval $[t, t + dt]$.

The rate of detachment Γ is defined as the ratio of the number of active strands that separate from temporary junctions per unit time to the total number of active strands. Applying this definition to active strands that were connected with the network at the initial instant $t=0$, and to those that merged with the network within the interval $[\tau, \tau + d\tau]$, we arrive at the differential equations

$$\frac{\partial n}{\partial t}(t, 0, v) = -\Gamma(v)n(t, 0, v), \quad \frac{\partial^2 n}{\partial t, \partial \tau}(t, \tau, v) = -\Gamma(v)\frac{\partial n}{\partial \tau}(t, \tau, v). \quad (8)$$

Integration of Eq. (8) with initial conditions Eqs. (6) (where we set $t=0$) and (7) implies that

$$n(t, 0, v) = N_{ap}(v)\exp[-\Gamma(v)t], \quad \frac{\partial n}{\partial t}(t, \tau, v) = \gamma(\tau, v)\exp[-\Gamma(v)(t-\tau)]. \quad (9)$$

To exclude the function $\gamma(t, v)$ from Eq. (9), we use the identity

$$n(t, t, v) = n(t, 0, v) + \int_0^t \frac{\partial n}{\partial t}(t, \tau, v)d\tau. \quad (10)$$

Substitution of expressions Eqs. (6) and (9) into Eq. (10) results in

$$N_{ap}(v) = N_{ap}(v)\exp[-\Gamma(v)t] + \int_0^t \gamma(\tau, v)\exp[-\Gamma(v)(t-\tau)]d\tau.$$

The solution of this equation reads $\gamma(t, v) = N_{ap}(v)\Gamma(v)$. Combining this expression with Eq. (9),

we find that

$$\frac{\partial n}{\partial \tau}(t, \tau, v) = N_a p(v) \Gamma(v) \exp[-\Gamma(v)(t - \tau)] \quad (11)$$

We adopt the conventional assumptions that (1) the excluded-volume effect and other multi-chain effects are screened for individual strands by surrounding macromolecules, (2) the energy of interaction between strands can be taken into account with the help of the incompressibility condition and (3) thermal oscillations of junctions can be disregarded, and the strain tensor for the motion of junctions at the microlevel coincides with the strain tensor for macro-deformation.

At isothermal deformation with small strains, a strand is treated as an isotropic incompressible medium. The strain energy of an active strand w_0 is determined by the conventional formula

$$w_0 = \mu \hat{e}' : \hat{e}',$$

where μ is an average elastic modulus of a strand, \hat{e} is the strain tensor for transition from the reference (stress-free) state of the strand to its deformed state, the prime stands for the deviatoric component of a tensor, and the colon denotes convolution of two tensors.

According to the affinity hypothesis, the strain energy $\bar{w}_0(t, 0)$ of an active strand that has not separated from the network during the interval $[0, t]$ reads

$$w(t, 0) = \mu \hat{\epsilon}'(t) : \hat{\epsilon}'(t),$$

where $\hat{\epsilon}(t)$ is the strain tensor for transition from the initial (stress-free) state of the network to its deformed state at time t . With reference to (Lodge 1968), we suppose that stress in a dangling strand totally relaxes before this strand captures a new junction. This implies that the stress-free state of an active strand that merges with the network at time $\tau \geq 0$ coincides with the deformed state of the network at that instant. The mechanical energy of an active strand that has last merged with the network at time $\tau \in [0, t]$ is given by

$$w(t, \tau) = \mu [\hat{\epsilon}(t) - \hat{\epsilon}(\tau)]' : [\hat{\epsilon}(t) - \hat{\epsilon}(\tau)]'.$$

Multiplying the strain energy per strand by the number of active strands per unit mass and summing the mechanical energies of active strands linked to temporary junctions with various activation energies, we find the strain energy per unit mass of an equivalent network

$$W(t) = \mu \int_0^\infty \left\{ n(t, 0, v) \hat{\epsilon}'(t) : \hat{\epsilon}'(t) + \int_0^t \frac{\partial n}{\partial \tau}(t, \tau, v) [\hat{\epsilon}(t) - \hat{\epsilon}(\tau)]' : [\hat{\epsilon}(t) - \hat{\epsilon}(\tau)]' d\tau \right\} dv. \quad (12)$$

Differentiating Eq. (12) with respect to time t and using Eqs. (9) to (11), we arrive at the formula

$$\frac{dW}{dt}(t) = \hat{A}'(t) : \frac{d\hat{\epsilon}'}{dt}(t) - B(t), \quad (13)$$

Where

$$\hat{A}(t) = 2\mu N_a \left\{ \hat{\epsilon}(t) - \int_0^t \hat{\epsilon}(T) dT \int_0^\infty \Gamma(v) \exp[-\Gamma(v)(t - \tau)] p(v) dv \right\}, \quad (14)$$

$$B(t) = \mu \int_0^\infty \Gamma(v) \left\{ n(t, 0, v) \hat{\epsilon}'(t) : \hat{\epsilon}'(t) + \int_0^t \frac{\partial n}{\partial \tau}(t, \tau, v) [\hat{\epsilon}(t) - \hat{\epsilon}(\tau)]' : [\hat{\epsilon}(t) - \hat{\epsilon}(\tau)]' d\tau \right\} dv \geq 0. \quad (15)$$

For isothermal deformation of an incompressible medium, the Clausius-Duhem inequality reads

$$Q = -\frac{dW}{dt} + \frac{\hat{\sigma}'}{\rho} : \frac{d\epsilon'}{dt} \geq 0,$$

where ρ is density, Q is internal dissipation per unit mass, and $\hat{\sigma}'$ stands for the stress tensor. Substitution of Eq. (13) into this equation implies that

$$Q(t) = \frac{1}{\rho} [\hat{\sigma}'(t) - \rho \hat{A}'(t)] : \frac{d\epsilon'}{dt}(t) + B(t) \geq 0. \quad (16)$$

As the function $B(t)$ is non-negative, see Eq. (15), the dissipation inequality Eq. (16) is satisfied, provided that the expression in the square brackets vanishes. This assertion together with Eq. (14) results in the constitutive equation

$$\hat{\sigma}(t) = -P(t)\hat{I} + 2G \left\{ \epsilon'(t) - \int_0^t \epsilon'(\tau) d\tau \int_0^\infty \Gamma(v) \exp[-\Gamma(v)(t-\tau)] p(v) dv \right\}, \quad (17)$$

where $P(t)$ is pressure, \hat{I} is the unit tensor, and $G = \rho\mu N_a$ is an analog of the shear modulus. Formula Eq. (17) describes the time-dependent response of an equivalent network at arbitrary three-dimensional deformations with small strains. In what follows, we confine ourselves to shear tests with

$$\hat{\epsilon}(t) = \epsilon(t)e_1e_2,$$

where $\epsilon(t)$ is the shear strain, and e_m ($m = 1, 2, 3$) are unit vectors of a Cartesian frame. According to Eq. (17), the shear stress $\sigma(t)$ is given by

$$\sigma(t) = 2G \left\{ \epsilon(t) - \int_0^t \epsilon(\tau) d\tau \int_0^\infty \Gamma(v) \exp[-\Gamma(v)(t-\tau)] p(v) dv \right\}. \quad (18)$$

It follows from Eq. (18) that in a shear oscillation test with

$$\epsilon(t) = \epsilon_0 \exp(i\omega t),$$

where ϵ_0 and ω are the amplitude and frequency of oscillations, and $i = \sqrt{-1}$, the transient complex modulus $\bar{G}^*(t, \omega) = \sigma(t)/(2\epsilon(t))$ is determined by the formula

$$\bar{G}^*(t, \omega) = G \left\{ 1 - \int_0^\infty \Gamma(v) p(v) dv \int_0^t \exp[-(\Gamma(v) + i\omega)s] ds \right\},$$

where $s = t - \tau$. The steady-state complex modulus $G^*(\omega) = \lim_{t \rightarrow \infty} \bar{G}^*(t, \omega)$ is given by

$$G^*(\omega) = G \int_0^\infty \frac{i\omega}{\Gamma(v) + i\omega} p(v) dv.$$

This equality together with Eq. (5) implies that the steady-state storage $G'(\omega)$ and loss $G''(\omega)$ shear moduli read

$$G'(\omega) = G \int_0^\infty \frac{\omega^2}{\Gamma_0^2 \exp(-2v) + \omega^2} p(v) dv, \quad G''(\omega) = G \int_0^\infty \frac{\Gamma_0 \exp(-v) \omega}{\Gamma_0^2 \exp(-2v) + \omega^2} p(v) dv. \quad (19)$$

To fit the experimental data, we adopt the random energy model (Ferry 1980) with the quasi-Gaussian distribution function $p(v)$,

$$p(v) = p_0 \exp\left[-\frac{(v-V)^2}{2\Sigma^2}\right] \quad (v \geq 0), \quad p(v) = 0 \quad (v < 0), \quad (20)$$

where V and Σ are adjustable parameters (the apparent average activation energy and the apparent standard deviation of activation energies, respectively), and the constant p_0 is found from the normalization condition

$$\int_0^{\infty} p(v) dv = 1. \quad (21)$$

Governing Eqs. (19) and (20) involve four material constants: (1) the instantaneous shear modulus G , (2) the attempt rate for rearrangement of strands Γ_0 , (3) an analog of the average activation energy for rearrangement of strands in a network V and (4) an analog of the standard deviation of activation energies Σ . When the dimensionless ratio $\xi = \Sigma / V$ is small compared to unity (it will be shown later that this condition is satisfied for our experimental data), the number of these parameters may be reduced to three. Assuming that

$$\xi \ll 1, \quad (22)$$

we can employ the first equality in Eq. (20) for an arbitrary (positive and negative) v . Replacing the lower limit of integration in Eq. (19) by $-\infty$, we obtain

$$G'(\omega) = Gp_0 \int_{-\infty}^{\infty} \frac{\omega^2}{\Gamma_0^2 \exp(-2v) + \omega^2} \exp\left[-\frac{(v-V)^2}{2\Sigma^2}\right] dv, \\ G''(\omega) Gp_0 \int_{-\infty}^{\infty} \frac{\Gamma_0 \exp(-v) \omega}{\Gamma_0^2 \exp(-2v) + \omega^2} \exp\left[-\frac{(v-V)^2}{2\Sigma^2}\right] dv, \quad (23)$$

where $p_0 = (\sqrt{2\pi}\Sigma)^{-1}$. To exclude the attempt rate Γ_0 from the consideration, we introduce the notation

$$\Gamma_0 = \Gamma_* \exp(v_0),$$

where Γ_* is a given value (in what follows, we set $\Gamma_* = 10^{10} s^{-1}$, which corresponds to the characteristic relaxation rate at the monomeric scale (Derrida 1980)), and $v_0 = \ln \Gamma_0 / \Gamma_*$. Substituting this expression into Eq. (23) and introducing the new variable $v' = v - v_0$, we find that

$$G'(\omega) = Gp_0 \int_{-\infty}^{\infty} \frac{\omega^2}{\Gamma_*^2 \exp(-2v') + \omega^2} \exp\left[-\frac{(v'-V')^2}{2\Sigma^2}\right] dv', \\ G''(\omega) = Gp_0 \int_{-\infty}^{\infty} \frac{\Gamma_* \exp(-v') \omega}{\Gamma_*^2 \exp(-2v') + \omega^2} \exp\left[-\frac{(v'-V')^2}{2\Sigma^2}\right] dv',$$

where $V' = V - v_0$. Omitting the primes for the sake of simplicity and replacing the lower limits of integration by zero, we return to Eq. (19), where the unknown attempt rate Γ_0 is replaced by Γ_* . This implies that each set of observations for the storage and loss shear moduli, $G'(\omega)$ and $G''(\omega)$, is entirely determined by three quantities: G , V and Σ . For a polymer melt subjected to thermal pre-treatment, these parameters are functions of annealing temperature T_a and annealing time t_a .

3.3 Fitting of observations

The constants G , V and Σ are found by matching separately each set of observations for $G'(\omega)$ and $G''(\omega)$ reported in Figs. 1, 2, 4, 5, 7 and 8. We fix some intervals $[0, V_{\max}]$ and $[0, \Sigma_{\max}]$, where the “best-fit” parameters V and Σ are assumed to be located, and divide these intervals into J subintervals by the points $V^{(i)} = i\Delta V$ and $\Sigma^{(j)} = j\Delta\Sigma$ ($i, j = 1, \dots, J-1$) with $\Delta V = V_{\max}/J$ and $\Delta\Sigma = \Sigma_{\max}/J$. For any pair $\{V^{(i)}, \Sigma^{(j)}\}$, the coefficient p_0 in Eq. (20) is calculated from Eq. (21), where the integral is evaluated numerically by Simpson's method with 400 points and the step $\Delta v = 0.1$. The integrals in Eq. (19) are calculated by using the same technique. The shear modulus G is found by the least-squares method from the condition of minimum of the function

$$F = \sum_{\omega_m} \{ [G'_{exp}(\omega_m) - G'_{num}(\omega_m)]^2 + [G''_{exp}(\omega_m) - G''_{num}(\omega_m)]^2 \},$$

where the sum is calculated over all experimental points ω_m , G'_{exp} and G''_{exp} are the storage and loss moduli measured in a test, and G'_{num} and G''_{num} are given by Eq. (19). The “best-fit” parameters V and Σ are determined from the condition of minimum of the function F on the set $\{V^{(i)}, \Sigma^{(j)}\}$. After finding the “best-fit” values $V^{(i)}$ and $\Sigma^{(j)}$, this procedure is repeated twice for the new intervals $[V^{(i-1)}, V^{(i+1)}]$ and $[\Sigma^{(j-1)}, \Sigma^{(j+1)}]$, to ensure an acceptable accuracy of fitting. Figs. 1, 2, 4, 5, 7 and 8 demonstrate good agreement between the experimental data and the results of numerical simulation.

For each annealing time t_a and annealing temperature T_a , we (1) find the ratio of mass-average molecular weights d_w from Eqs. (1) and (2) and the observations depicted in Figs. 3, 6 and 9, (2) calculate the material constants G , V and Σ by matching the experimental data plotted in Figs. 1, 2, 4, 5, 7 and 8 and (3) present the quantities G , V and Σ as functions of d_w .

The instantaneous shear modulus G is plotted versus the ratio of mass-average molecular weights d_w in Fig. 15 for LLDPE and in Fig. 16 for iPP. The experimental data are fitted by the linear equation

$$G = G_0 + G_1 d_w, \quad (24)$$

where the coefficients G_i ($i = 0, 1$) are calculated by the least-squares technique. Figs. 15 and 16 show that Eq. (24) provides an acceptable approximation of the observations. To compare our findings for LLDPE and iPP, we present Eq. (24) in the form

$$G = G_* [1 - Z_G (1 - d_w)],$$

where $G_0 = G_* (1 - Z_G)$ and $G_1 = G_* Z_G$. The coefficient Z_G is calculated by using the experimental data presented in Figs. 15 and 16. We find that $Z_G = 2.00$ for LLDPE and $Z_G = 0.61$ for iPP. This implies that the influence of molecular weight on the elastic modulus G is substantially more pronounced for linear low-density polyethylene than for isotactic polypropylene.

The dimensionless average activation energy for separation of strands from temporary junctions V is plotted versus the ratio of mass-average molecular weights d_w in Fig. 16 for LLDPE and in Fig. 17 for iPP. The experimental data are approximated by the constants,

$$V = V_0. \quad (25)$$

Figs. 17 and 18 show that the average activation energy for rearrangement of chains is independent of molecular weight. It is worth noting that the values of V for two polymer melts

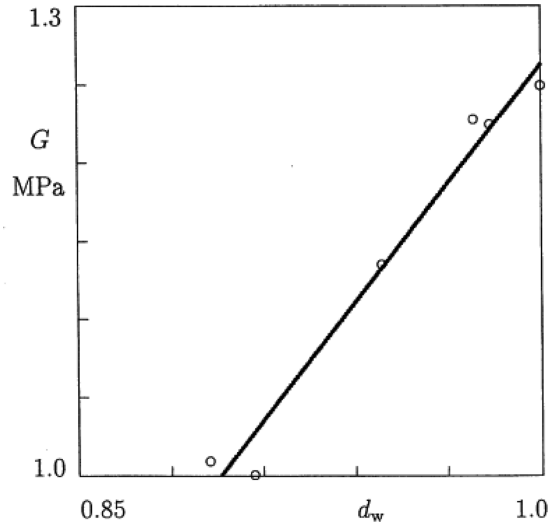


Fig. 14 The instantaneous shear modulus G versus the ratio of mass-average molecular weights d_w . Circles: treatment of observations in torsional oscillation tests on LLDPE. Solid line: approximation of the experimental data by Eq. (24) with $G_0 = -1.27$ and $G_1 = 2.53$

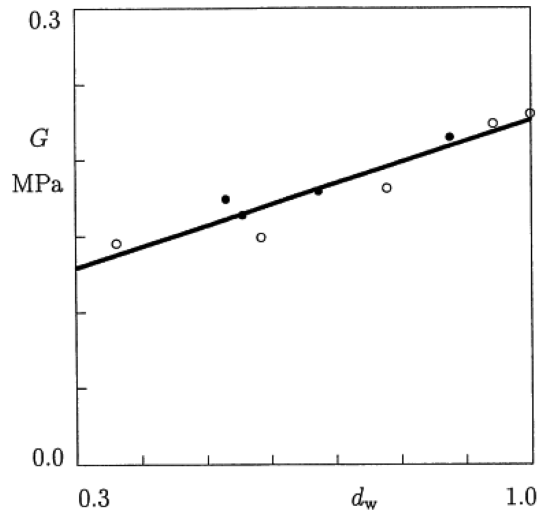


Fig. 15 The shear modulus G versus the ratio of mass-average molecular weights d_w . Symbols: treatment of observations in torsional oscillation tests at $T = 230^\circ\text{C}$ on iPP annealed for $t_a = 60$ min at the temperatures $T_a = 250, 270, 290$ and 310°C (unfilled circles) and annealed at the temperature $T_a = 190^\circ\text{C}$ for $t_a = 0, 30, 60, 90$ and 120 min (filled circles). Solid line: approximation of the experimental data by Eq. (24) with $G_0 = 0.087$ and $G_1 = 0.14$

cannot be compared directly with one another, because the rheological tests were performed at various temperatures, while the same value of Γ_* was employed in the fitting procedure.

The dimensionless standard deviation of activation energies Σ is depicted in Fig. 16 for LLDPE and in Fig. 17 for iPP. The observations are matched by the linear function.

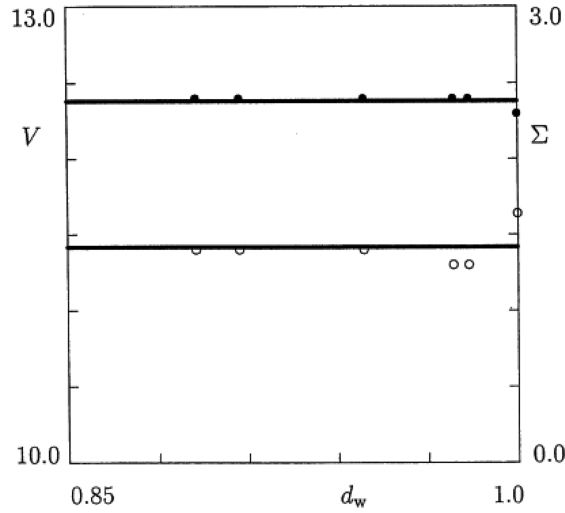


Fig. 16 The average activation energy V (unfilled circles) and the standard deviation of activation energies Σ (filled circles) versus the ratio of mass-average molecular weights d_w . Symbols: treatment of observations in torsional oscillation tests on LLDPE. Solid lines: approximation of the experimental data by Eqs. (25) and (26) with $V_0 = 11.42$, $\Sigma_0 = 2.38$ and $\Sigma_1 = 0$

$$\Sigma = \Sigma_0 + \Sigma_1 d_w, \quad (26)$$

where the coefficients Σ_i ($i = 0,1$) are found by the least-squares algorithm. Figs. 16 and 17 demonstrate that the mass-average molecular weight affects the standard deviation of activation energies of LLDPE and iPP in different ways. The parameter Σ is independent of d_w for linear low-density polyethylene, and Σ strongly grows with mass-average molecular weight for isotactic polypropylene.

According to Figs. 16 and 17, the ratio ξ does not exceed 0.2 for both polymer melts under consideration, which implies that inequality Eq. (22) is satisfied with a reasonable level of accuracy.

4. Discussion

We begin with the analysis of material constants in Eq. (1) that describes the effect of frequency of oscillations ω on the modulus of complex viscosity η . According to Figs. 10 and 11, the exponent α decreases with molecular weight for both polymers. Changes in the function $\alpha(d_w)$ are rather modest: the values of α are located in the interval between 0.6 and 0.9 for LLDPE and in the interval between 0.4 and 0.8 for iPP (not far away from the value $\alpha = 2/3$ conventionally used in matching observations). According to Eq. (3), the rate of decrease in α with d_w for LLDPE exceeds that for iPP, which means that the presence of highly branched chains in a polymer melt reduces the influence of molecular weight on this quantity.

Figs. 12 and 13 reveal a substantial difference between the effects of molecular weight on the characteristic time τ of two polyolefins. According to Fig. 13, τ increases with d_w for polypropylene melt. This behavior appears to be quite natural, as it resembles in some sense the influence on mass-average molecular weight M_w on the zero-frequency viscosity η_0 , see Eq. (2). The increase in

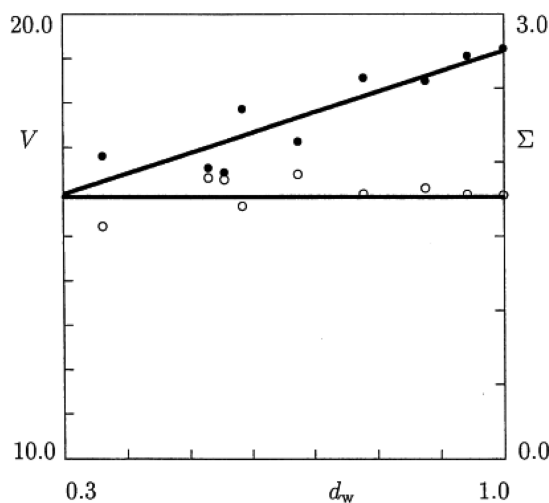


Fig. 17 The average activation energy V (unfilled circles) and the standard deviation of activation energies Σ (filled circles) versus the ratio of mass-average molecular weights d_w . Symbols: treatment of observations in torsional oscillation tests on iPP. Solid lines: approximation of the experimental data by Eqs. (25) and (26) with $V_0 = 15.88$, $\Sigma_0 = 1.37$ and $\Sigma_1 = 1.39$

T with molecular weight observed for iPP is also in agreement with the reptation concept that predicts a similar behavior (Doi 1986).

Fig. 12 shows that the characteristic time T strongly decreases with M_w for polyethylene melt. The scatter of the experimental data in Fig. 13 is relatively small. Deviations of the observations depicted in Fig. 12 from their approximation by Eq. (3) are a bit larger, but even they are too small to suppose that other characteristics of molecular weight (like, for example, the polydispersity index (Carrot 1996)) may noticeably affect τ .

To provide some explanation for the unusual decrease in the characteristic time of LLDPE with molecular weight, we recall that the growth of relaxation time with molecular weight is conventionally attributed to curvilinear diffusion of a characteristic chain along a tube formed by surrounding macromolecules (Doi 1986). The latter implies that the larger the average length of a chain is, the higher is the disengagement time (the time necessary for the chain to leave the home tube). This conclusion, however, remains true, provided that the average radius of the tube is unaffected by changes in molecular weight. In our recent study on the kinetics of thermal degradation ((Drozdov 2003), it was demonstrated that the evolution of molecular weight driven by the degradation process may be adequately described as a combination of two processes: binary scission (fragmentation) of chains, and detachment and subsequent diffusion and evaporation (annihilation) of side-groups and short branches. It is natural to suppose that for a polymer melt with long-branched chains (iPP), the annihilation process weakly affects the radius of a tube to which the characteristic chain is confined, because this radius is mainly determined by the architecture of long branches that prevent chains to shrink. On the contrary, annihilation of side-groups and short branches in a network of short-branched chains (LLDPE) should result in a substantial decrease in the radius of a tube, and, as a consequence, in a noticeable increase of the reptation time, in agreement with the observations depicted in Fig. 12.

To add some quantitative estimates to this qualitative description, we determine the characteristic

time T by the conventional formula (Drozdov 2003)

$$\tau = \Gamma_*^{-1} M_n^3 \left(1 - \sqrt{\frac{M_e}{M_n}} \right)^2, \quad (27)$$

where M_n is the number-average molecular weight and M_e is the molecular weight between entanglements. It follows from Eq. (27) that T can increase with a decrease in molecular weight, provided that the molecular weight between entanglements M_e grows with the number average molecular weight M_n rather rapidly,

$$\frac{d\lambda}{dM_n} > \frac{3}{2M_n}(1-\lambda), \quad (28)$$

where $\lambda = \sqrt{M_e/M_n}$.

Figs. 14 and 15 reveal that the elastic modulus G linearly increases with mass-average molecular weight. This conclusion is in agreement with the classical theory of rubber elasticity (Ferry 1980), according to which the shear modulus is proportional to the molecular weight between entanglements M_e , which, in turn, grows to molecular weight. It is worth noting that the influence of d_w on G is more pronounced for LLDPE than for iPP. This conclusion seems rather natural, because annihilation of side-groups and short branches at thermal degradation of polyethylene melt strongly enhances disentanglement of chains. It is also in accord with estimate Eq. (28), which implies that the molecular weight between entanglements of LLDPE increases more rapidly with molecular weight than that of iPP.

Figs. 16 and 17 show that the average activation energy for separation of strands from temporary junctions V is not affected by molecular weight. This finding may be treated as an indirect confirmation of the model, because the energy V characterizes local interactions between two entangled chains which are not affected by their lengths.

According to Figs. 16 and 17, the effect of molecular weight on the standard deviation of activation energies Σ of LLDPE and iPP is quite different. For linear low-density polyethylene, Σ remains independent of mass-average molecular weight, whereas for isotactic polypropylene, Σ linearly grows with d_w . This result seems natural as well. Indeed, it follows from Eq. (20) that Σ serves as a measure of disorder in the distribution of activation energies that reflects different strengths of interaction between strands in an equivalent network. For a network of linear chains with short branches (LLDPE), fragmentation of chains induced by thermal degradation does not cause substantial changes in the strength of interaction, which implies that Σ remains constant. On the contrary, for a network of highly branched chains (iPP), thermal degradation induces fragmentation of chains at the branching points, which implies that the content of junctions with high energies of interaction is reduced, and, as a consequence, the width of the distribution of activation energies decreases, in accord with the observations presented in Fig. 17.

5. Conclusions

Two series of torsional oscillation tests with small strains have been performed on linear low density polyethylene at the temperature $T = 140^\circ\text{C}$ and isotactic polypropylene at $T = 230^\circ\text{C}$. Prior to rheological testing, specimens were annealed at various temperatures T_a (from 180 to 310°C) for

various amounts of time t_a ranging from 30 to 120 min. Thermal treatment induced thermal degradation of samples observed as a pronounced decrease in their mass average molecular weight with exposure time t_a .

A constitutive model has been developed for the viscoelastic response of a polymer melt at isothermal three-dimensional deformations with small strains. The melt is treated as an equivalent transient network of strands bridged by temporary junctions. Its time-dependent behavior is modeled as separation of active strands from their junctions and attachment of dangling strands to the network. The rearrangement events occur at random times, as appropriate strands are thermally activated.

Stress-strain relations for an equivalent heterogeneous network of strands (where different junctions have different activation energies for rearrangement of strands) have been derived by using the laws of thermodynamics. The constitutive equations involve three material parameters that are determined by matching the experimental data for the storage and loss moduli as functions of frequency of oscillations. Fair agreement is demonstrated between the observations and the results of numerical simulation.

The following conclusions are drawn; The characteristic time for relaxation T decreases with molecular weight for LLDPE and increases for iPP. For both polymers under consideration, the average activation energy for rearrangement of strands V is independent of molecular weight. The shear modulus G linearly grow with mass-average molecular weight M_w . The standard deviation of activation energies Σ is independent of mass-average molecular weight for LLDPE and linearly grows with M_w for iPP.

References

- Barakos, G., Mitsoulis, E., Tzoganakis, C. and Kajiwara, T. (1996), "Rheological characterization of controlled-rheology polypropylenes using integral constitutive equations", *J. Appl. Polym. Sci.*, **59**(3), 543-556.
- Berzin, F., Vergnes, B. and Delamare, L. (2001), "Rheological behavior of controlled-rheology polypropylenes obtained by peroxide-promoted degradation during extrusion: Comparison between homopolymer and copolymer", *J. Appl. Polym. Sci.*, **80**(8), 1243-1252.
- Carrot, C., Revenu, P. and Guillet, J. (1996), "Rheological behavior of degraded polypropylene melts: From MWD to dynamic moduli", *J. Appl. Polym. Sci.*, **61**(11), 1887-1897.
- Combs, R.L., Slonaker, D.F. and Coover, H.W. (1969), "Effects of molecular weight distribution and branching on rheological properties of polyolefin melts", *J. Appl. Polym. Sci.*, **13**(3), 519-534.
- Derrida, B. (1980), "Random-energy model: Limit of a family of disordered models", *Phys. Rev. Lett.*, **45**(2), 79-82.
- Dlubek, G., Bamford, D., Rodriguez-Gonzalez, A., Bornemann, S., Stejny, J., Schade, B., Alam, M.A. and Arnold, M. (2002), "Free volume, glass transition, and degree of branching in metallocene-based propylene/ α -olefin copolymers: Positron lifetime, density, and differential scanning calorimetric studies", *J. Polym. Sci. Pol. Phys.*, **40**(5), 434-453.
- Doi, M. and Edwards, S.F. (1986), *The theory of polymer dynamics*, Oxford University Press, New York.
- Drozdov, A.D. and Christiansen, J.D. (2003), "The effect of annealing on the nonlinear viscoelastic response of isotactic polypropylene", *Polym. Eng. Sci.*, **43**(4), 946-959.
- Drozdov, A.D. and Christiansen, J.D. (2003), "The effect of annealing on the elastoplastic and viscoelastic responses of isotactic polypropylene", *Comp. Mater. Sci.*, **27**(4), 403-422.
- Drozdov, A.D., Agrawal, S. and Gupta, R.K. (2005), "The effect of temperature on the viscoelastic response of polymer melts", *Int. J. Eng. Sci.*, **43**(3-4), 304-320.
- Drozdov, A.D. and Yuan, Q. (2003), "The viscoelastic and viscoplastic behavior of low-density polyethylene",

- Int. J. Solids Struct.*, **40**(10), 2321-2342.
- Drozdov, A.D. and Yuan, Q. (2003), "Effect of annealing on the viscoelastic and viscoplastic responses of low-density polyethylene", *J. Polym. Sci. Pol. Phys.*, **41**(14), 1638-1655.
- Drozdov, A.D. (2003), "Kinetic equations for thermal degradation of polymers", *arXiv:cond-mat/0309677v1 [cond-mat.mtrl-sci]*.
- Eckstein, A., Friedrich, C., Lobbrecht, A., Spitz, R. and Mülhaupt, R. (1997), "Comparison of the viscoelastic properties of syndio- and isotactic polypropylenes", *Acta Polym.*, **48**(1-2), 41-46.
- Fayolle, B., Audouin, L. and Verdu, J. (2002), "Initial steps and embrittlement in the thermal oxidation of stabilised polypropylene films", *Polym. Degrad. Stabil.*, **75**(1), 123-129.
- Ferry, J.D. (1980), *Viscoelastic properties of polymers*, 3rd Ed., Wiley, New York.
- Fujiyama, M., Kitajima, Y. and Inata, H. (2002), "Rheological properties of polypropylenes with different molecular weight distribution characteristics", *J. Appl. Polym. Sci.*, **84**(12), 2128-2141.
- Fujiyama, M. and Inata, H. (2002), "Rheological properties of metallocene isotactic polypropylenes", *J. Appl. Polym. Sci.*, **84**(12), 2157-2170.
- Gao, J.M., Lu, Y.J., Wei, G.S., Zhang, X.H., Liu, Y.Q. and Qiao, J.L. (2002), "Effect of radiation on the crosslinking and branching of polypropylene", *J. Appl. Polym. Sci.*, **85**(8), 1758-1764.
- Gao, Z., Kaneko, T., Amasaki, I. and Nakada, M. (2003), "A kinetic study of thermal degradation of polypropylene", *Polym. Degrad. Stabil.*, **80**(2), 269-274.
- Genies, P.G. (1979), *Scaling concepts in polymer physics*, Cornell University Press, Ithaca, N.Y.
- Graessley, W. (1982), "Entangled linear, branched and network polymer systems — Molecular theories", *Adv. Polym. Sci.*, **47**, 67-117.
- Green, M.S. and Tobolsky, A.V. (1946), "A new approach to the theory of relaxing polymeric media", *J. Chem. Phys.*, **14**(2), 80-92.
- Horrocks, A.R., Valinejad, K. and Crighton, J.S. (1994), "Demonstration of the possible competing effects of oxidation and chain scission in orientated and stressed polypropylenes", *J. Appl. Polym. Sci.*, **54**(5), 593-600.
- Iijima, M. and Strobl, G. (2000), "Isothermal crystallization and melting of isotactic polypropylene analyzed by time- and temperature-dependent small-angle X-ray scattering experiments", *Macromolecules*, **33**(14), 5204-5214.
- Kim, Y.C., Yang, K.S. and Choi, C.H. (1998), "Study of the relationship between shear modification and melt fracture in extrusion of LDPE", *J. Appl. Polym. Sci.*, **70**(11), 2187-2195.
- Kim, M.H., Londono, J.D. and Habenschuss, A. (2000), "Structure of molten stereoregular polyolefins with different side-chain sizes: Linear polyethylene, polypropylene, poly(1-butene), and poly(4-methyl-1-pentene)", *J. Polym. Sci. Pol. Phys.*, **38**, 2480-2485.
- Kumar, G.S., Kumar, V.R. and Madras, G. (2002), "Continuous distribution kinetics for the thermal degradation of LDPE in solution", *J. Appl. Polym. Sci.*, **84**(4), 681-690.
- Lodge, A.S. (1968), "Constitutive equations from molecular network theories for polymer solutions", *Rheol. Acta*, **7**(4), 379-392.
- Matsuda, H., Aoike, T., Uehara, H., Yamanobe, T. and Komoto, T. (2001), "Overlapping of different rearrangement mechanisms upon annealing for solution-crystallized polyethylene", *Polymer*, **42**(11), 5013-5021.
- Mäder, D., Heinemann, J., Walter, P. and Mülhaupt, R. (2000), "Influence of n-alkyl branches on glass-transition temperatures of branched polyethylenes prepared by means of metallocene- and palladium-based catalysts", *Macromolecules*, **33**(4), 1254-1261.
- Pérez, C.J., Cassano, G.A., Vallés, E.M., Quinzani, L.M. and Failla, M.D. (2003), "Tensile mechanical behavior of linear high-density polyethylenes modified with organic peroxide", *Polym. Eng. Sci.*, **43**(9), 1624-1633.
- Rangarajan, P., Bhattacharyya, D. and Grulke, E. (1998), "HDPE liquefaction: Random chain scission model", *J. Appl. Polym. Sci.*, **70**(6), 1239-1251.
- Sugimoto, M., Masubuchi, Y., Takimoto, J. and Koyama, K. (2001), "Melt rheology of polypropylene containing small amounts of high molecular weight chain. I. Shear flow", *J. Polym. Sci. Pol. Phys.*, **39**(21), 2692-2704.
- Sugimoto, M., Masubuchi, Y., Takimoto, J. and Koyama, K. (2001), "Melt rheology of polypropylene containing small amounts of high-molecular-weight chain. 2. uniaxial and biaxial extensional flow", *Macromolecules*, **34**(17), 6056-6063.

- Sweeney, J., Collins, T.L.D., Coates, P.D. and Duckett, R.A. (1999), "High-temperature large strain viscoelastic behavior of polypropylene modeled using an inhomogeneously strained network", *J. Appl. Polym. Sci.*, **72**(4), 563-575.
- Tanaka, F. and Edwards, S.F. (1992), "Viscoelastic properties of physically cross-linked networks - transient network theory"; *Macromolecules*, **25**(5), 1516-1523.
- Tiemblo, P., Gómez-Elvira, J.M., Beltrán, S.G., Matisova-Rychla, L. and Rychly, J. (2002), "Melting and Relaxation Effects on the Kinetics of Polypropylene Thermooxidation in the Range 80-170°C", *Macromolecules*, **35**(15), 5922-5926.
- Van Prooyen, M., Bremner, T. and Rudin, A. (1994), "Mechanism of shear modification of low density polyethylene", *Polym. Eng. Sci.*, **34**(7), 570-579.
- Wang, X., Tzoganakis, C. and Rempel, G. L. (1996), "Chemical modification of polypropylene with peroxide/pentaerythritoltriacylate by reactive extrusion", *J. Appl. Polym. Sci.*, **61**(8), 1395-1404.
- Yamamoto, M. (1956), "The visco-elastic properties of network structure I. general formalism", *J. Phys. Soc. Jpn.*, **11**(4), 413-421.